Cleaner Logistics and Supply Chain 3 (2022) 100022

Contents lists available at ScienceDirect

Cleaner Logistics and Supply Chain

journal homepage: www.elsevier.com/locate/clscn

Electric vehicle sharing based “energy sponge” service interfacing transportation and power systems

Qianwen Li [a], Dongfang Zhao [a], Xiaopeng Li [a,*], Xin Wang [b]

[a] Department of Civil and Environmental Engineering University of South Florida, Tampa, FL 33620, United States
[b] Industrial and Systems Engineering, University of Wisconsin-Madison, WI 53706, United States

ARTICLE INFO

Keywords:
Electric vehicle (EV)
Shared mobility
Power systems
Fleet management
Dynamic programming

ABSTRACT

Electrical vehicles (EVs) by the nature of the technology assume a dual role of supplying transportation mobility and storing electric power. Thus, the operations of EV impact both transportation and power grid systems. This study proposes the concept of an “energy sponge” service by de- signing an EV sharing system serving both a transportation system and a power market. The proposed model investigates operations of a fleet of EVs that may opt to serve the transportation system when the transportation demand is high or return electricity to the grid when the power price shoots high. A Markov decision model is proposed to determine the optimal policy on time allocation of the EV fleet over the two systems. A dynamic programming algorithm is developed to solve the model efficiently. Real-world data on the configurations of these two markets are used to build numerical examples. Sensitivity analyses are constructed to draw insights into the benefits and operational patterns of the service. Overall, this model provides methods and insights for EV fleet managers to decide optimal policies for allocating the EV fleet between transportation and power markets. Besides shared mobility systems, this model also has great potential in other logistics and supply chain systems where EVs are used to deliver goods or services.

1. Introduction and literature review

Mobility service paradigms have experienced drastic transformations in recent years. In particular, shared mobility service, recognized as the missing link to sustainable transportation (Britton, 2000; Bardaka et al., 2020), integrates flexibility, mobility, and accessibility from private vehicles and economy and sustainability from public transit. Shared mobility has tremendous impacts on the environment and society, e.g., reducing total vehicle fleets and individual ownership costs (Martin et al., 2010) and possibly lowering vehicle kilometers traveled and greenhouse gas (GHG) emissions Martin and Shaheen (2011). Due to these advantages, the car-sharing service market has surpassed USD 2 billion in 2020 across the world (Gminsights, 2020). Successful car-sharing business cases include Autolib, JustShareIt, and Zipcar. Moreover, ridesharing has been booming in recent years as evidenced by the rapid successes of mega transportation network companies, including Uber, Lyft, and Didi.

In conjunction with mobility service shifts, vehicle technologies have gone through several revolutions, one of which as particularly highlighted in recent years is electrification Quddus et al. (2019); Guo et al. (2017). Electrical vehicles (EVs) have grown rapidly in recent years, primarily due to their low operating costs, high energy efficiency (Thiel et al., 2010), and reduced emission pollutants (Juul and Meibom, 2011). The number of global EVs has increased from 1.2 million to 6.8 million in the past five years (Statista, 2020). Based on the forecast by Becker et al. (2009), by 2030, EVs will account for 64% of U.S. light-vehicle sales, comprise 24% of the U.S. light-vehicle fleet, and result in a 20–69% decline in GHG from U.S. light-vehicles. Intensive research efforts have been made recently in several directions including charging station deployment (Asamer et al., 2016; Chen et al., 2016b; Yi and Bauer, 2016; Tu et al., 2016; Li et al., 2016a; Huang et al., 2015; Li et al., 2016b) and joint routing and charging operations (Wang et al., 2017; He et al., 2014; Alizadeh et al., 2014; Yin et al., 2009; Ukkusuri et al., 2007; Gardner et al., 2013; Siddiqi et al., 2011) for EV systems. Due to these advantages, several shared mobility systems (e.g., Uber and Zipcar) have adopted EVs in their vehicle fleets. This paper will focus on operational policies for an electric vehicle sharing system.

Operations of a shared mobility system are largely affected by transportation demand fluctuations over time. On the one hand, the

* Corresponding author.
E-mail address: xiaopengli@usf.edu (X. Li).

https://doi.org/10.1016/j.clscn.2021.100022
Received 17 November 2021; Accepted 14 December 2021

idle time of shared vehicles decreases with the demand level increase, and a higher demand usually means higher utilization rates of shared vehicles. Therefore, demand variations usually lead to revenue fluctuations. On the other hand, demand variations are often associated with surge pricing that is particularly prevailing in the shared mobility market (Bai et al., 2017; Cachon et al., 2017; Guda and Subramanian, 2017; Taylor, 2017; Bimpikis et al., 2016; Gardner et al., 2010), i.e., higher transportation demand often triggers higher unit transportation price Nie and Liu (2010). Obviously, in addition to demand-volume-induced profit changes, surge pricing further amplifies revenue fluctuations of a shared mobility system. For example, the 20-minute revenue per vehicle in the New York taxi system varies widely between $4.5 and $8.5, as Fig. 1 shows.

Note that a large fleet of shared vehicles is actually EVs, simply because the environmental and social benefits of shared mobility can be further enhanced by the above-stated advantages (Green, 2009; Ford, 1995). Operations of EV sharing have drawn increasing attention from researchers, and a number of studies on this topic have been conducted (He et al., 2013; Asamer et al., 2016; Chen et al., 2016a; Yi and Bauer, 2016; Tu et al., 2016; Li et al., 2016a; Huang et al., 2015). EVs, as massive “moving batteries”, also have a huge potential of serving the power market, particularly when they are subject to centralized dispatches in a shared mobility system. In fact, the power market is in great need of ancillary power supplies, primarily due to frequent and wide power price oscillations over the course of the day. Fig. 1 shows an example of power price variations over the course of a day in New York City. We see that the price changes rapidly across different hours. Therefore, it might be profitable to charge EVs from the grid during an off-peak price time and discharge them to the grid during a peak price time, as referred to in the vehicle-2-grid (V2G) technology (Sundstrom and Binding, 2012; Gao et al., 2014; Parsons et al., 2014; Sovacool et al., 2017; Chen et al., 2016a). Researchers outside of transportation engineering have investigated this opportunity of regulating EV charging and discharging activities to capitalize on power price variations in recent years (Du et al., 2016; He et al., 2012; Cao et al., 2012; Koyanagi and Uriu, 1998; Ortega-Vazquez et al., 2013). The integration of transportation services and ancillary power supply in an EV sharing system is relatively new. It is an indisputable fact that EVs assume a dual role of both supplying transportation mobility and storing electric power, and thus hold promise for composing an “energy sponge” service interfacing with both transportation and power grid systems. By examining fluctuations in transportation revenue and electricity rates (Fig. 1, some interesting complementary patterns

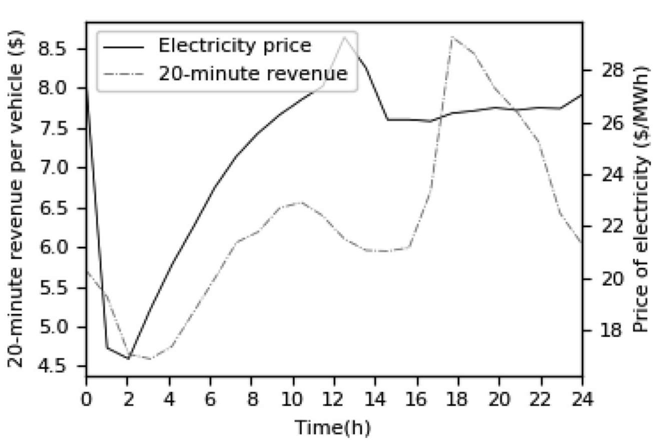

Fig. 1. 20-minute revenue per vehicle of the New York City taxi system in 01/01/2016 (NYC, 2016) and electricity rates in New York City in 01/01/2016 (Pjm, 2016).

are observed during certain time intervals. For example, in the afternoon, the power price is relatively low and the transportation revenue has high spikes, and thus the EV sharing system can opt to serve the transportation system for a possible higher profit during this time. Whereas in the evening, the power price has ramped up while the transportation revenue declines to a low level, and the EV sharing system can switch to the power market (i.e., discharging to the grid) instead. By dynamically switching between the two markets, the EV sharing system not only maximizes its own profit but also balances service and resource supplies in both markets for better overall social welfare. Ren et al.(2019) predicted station-level travel demand and proposed an electric vehicle sharing network to address the vehicle unbalancing issue while satisfying vehicle charging and discharging needs. Zhang et al. (2021) constructed a space-time-electricity-expanded transportation network and optimized the operations of shared electric vehicle fleets. Different operations were incorporated including serving travel demand, rebalancing vehicle distribution, staying idle, charging, and discharging. Jiao et al. (2021) investigated a robust model to optimize electric vehicle charging and discharging schedules. With a distributed framework, the proposed model addressed operational uncertainties, e.g., travel demand, without requiring the full data distribution. Caggiani et al. (2021) developed an electric vehicle relocation strategy considering vehicle charging and discharging operations in a vehicle-to-grid framework. While the existing studies provide insights in devising shared EV operations, they usually assume a deterministic electricity price. This assumption makes the problem tractable yet cannot capture the stochastic nature of the electricity price. The resulting model is not realistic and the findings may be impractical. As a result, a stochastic approach is needed to address this limitation.

This paper proposes an “energy sponge” concept and implements it in an EV sharing system. This investigated problem is deciding the optimal time allocations of a fleet of shared EVs on the transportation system and the power market to maximize the total profit while considering the electricity price stochasticity. This problem is formulated into a Markov decision problem (MDP) and we solve this problem with an efficient dynamic programming (DP) algorithm (Mahmoudi and Zhou, 2016). We also propose a data-driven approach to extract input parameters from real-world taxi data and power price logs. With this approach, numerical examples are constructed based on real-world taxi trip data and power price history in New York City. These examples are solved with both Gurobi, a commercial integer programming solver, and the proposed DP algorithm. The results show that while the Gurobi takes a relatively long solution time (e.g., tens of minutes) and often cannot obtain the exact solution within the time limit, DP always solves the exact optimum in a very short time (e.g., at most a few seconds). Sensitivity analysis is also conducted to examine how the solution changes with variations of key parameters. The outcomes from this study provide useful methods and interesting insights into allocating an EV fleet between the transportation and power markets, which will be helpful to fleet managers in determining the most profitable policies in EV operations. Further, the interface between transportation and power will increase the profitability of the service, e.g., by over 40% in nominal conditions. Although this study focuses on optimizing the operation of shared EV fleets, the proposed methodology is not limited to solving EV sharing problems, it also has great potential in other logistics and supply chain systems where EVs are used to deliver goods or services.

The remainder of the paper is organized as follows. Section 2 describes the problem setting and formulates the integer programming model. Section 3 describes the dynamic programming algorithm for solving the proposed model. Section 4 proposes the parameter extraction methods and conducts numerical examples with real-world data. Section 5 concludes the paper and discusses possible future research directions.

2. General problem formulation

For the convenience of the readers, the major parameters and variables in this study are listed in Table 1. We consider a problem of managing an EV fleet in a finite operational horizon of I time points, indexed as $\mathscr{I} = \{1, 2, ..., I\}$. For example, $\mathscr{I}$ can be a day with 24 hourly time points, i.e., $i \in \mathscr{I} = \{1, 2, ..., 24\}$. At each time point $i \in \mathscr{I}$, we need to decide whether to let the fleet serve the transportation system, charge from the power grid (to recover the SoC), discharge to the power grid (to gain revenue from selling electricity to the grid), or stay idle, as illustrated in Fig. 2. Note that we view the fleet as a whole unit and we do not consider the split of the vehicles across different markets (or states) at the same time interval. Although this setting may lose some optimality of the operational revenue as opposed to individual vehicle decisions, it helps the analysis focus on the concept of the "energy sponge" service and draws insights into relevant operational policies. Let L denote the initial full state of charge (SoC) of the EV fleet and f_i denote the fleet SoC at each time point i.

Without loss of generality, we only consider integer SoC levels. In this study, we assume that the availability of EV charging/discharging stations is high, and the access time to a station anytime anywhere is negligible compared to a time interval duration. With this, the cost/revenue from charging/discharging decisions are additive across time points. Following most practices, we assume that the fleet SoC is L at the beginning and the end of the operational horizon (e.g., a day) and it has to be maintained between 0 and L during the horizon. Let d^+ denote the EV charging rate for every time interval $[i, i+1], \forall i \in \mathscr{I}$; i.e., the vehicle's fleet SoC fi will raise by d^+ after being charged for a time interval $[i, i+1], \forall i \in \mathscr{I}$ until reaching full SoC L. We consider a time-varying and stochastic EV charging cost that is assumed to be known at the beginning. Denote the cost to charge the fleet during the time interval $[i, i+1], \forall i \in \mathscr{I}$ as c_i. We assume that c_i follow a Poisson distribution: $c_i \sim \lambda_i^c, P(c_i = k) = \left(\left(\lambda_i^c\right)^k e^{-\lambda_i^c} \right)/k!$, $k \in [1, \cdots, \infty]$, where λ_i^c denotes the expected cost of charging during the time interval $[i, i+1], \forall i \in \mathscr{I}$. Similarly, we let d^- denote the SoC decreasing rate for every time interval $[i, i+1], \forall i \in \mathscr{I}$ when the EV fleet is put to serve the power grid by discharging electricity to the grid. Let s_i denote the stochastic revenue of discharging from time point i to time point $i+1$ or during the time interval $[i, i+1], \forall i \in \mathscr{I}$. Again, we assume that the revenue of discharging s_i follows a Poisson distribution $s_i \sim \lambda_i^s, P(s_i = k) = \left(\left(\lambda_i^s\right)^k e^{-\lambda_i^s} \right)/k!, k \in [1, \cdots, \infty)$ where λ_i^s denotes the expected revenue of discharging during the time interval $[i, i+1], \forall i \in \mathscr{I}$.

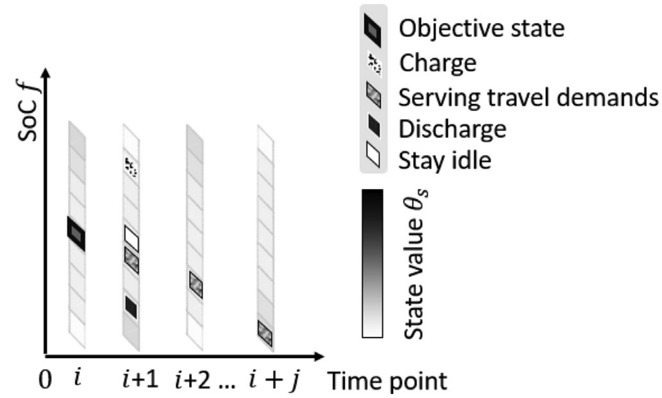

Fig. 2. State of the proposed network.

Further, when we decide to dispatch the EV fleet to serve travel demands, note that the corresponding revenue, unlike the discharging service, is not necessarily additive across time intervals. This is because some trips in the transportation system may be comparable or longer than one time interval $[i, i+1], \forall i \in \mathscr{I}$, which will restrict the trips the fleet can serve if the fleet is allocated to the transportation system just for a short period. Further, the waiting times in between trips may also affect the revenue. Therefore, the average revenue per time interval might be different across different service durations, and thus the transportation revenue cannot be simply separated and become independent across time intervals as the discharging revenue. To address this issue, we define a specific revenue for each possible service duration for travel demands in a transportation system. Let $\mathscr{J}_i := \{1, 2, 3, ..j, ..., min\{J, I-i\}\}$ be the set of all possible service durations at time point i. J can be set to a number such that most trip durations are much less than J time intervals, and at the scale of this duration, the revenue of serving travel demands can be separated without much error. Define d_{ij} and b_{ij} as the corresponding energy consumption and the stochastic revenue to serve travel demands starting from time point i to time point $i+j$, or during the time interval $[i, i+j]$. Similarly, we assume that the revenue of serving travel demands b_{ij} follows a Poisson distribution: $b_{ij} \sim \lambda_{ij}^b, P(b_{ij} = k) = \left(\left(\lambda_{ij}^b\right)^k e^{-\lambda_{ij}^b} \right)/k!$, $k \in [1, \cdots, \infty)$, where λ_{ij}^b denotes the expected revenue of serving travel demands during the time interval $[i, i+j], \forall i+j \in \mathscr{I}, \forall i \in \mathscr{I}, \forall j \in \mathscr{J}$.

To establish an MDP model, we firstly define the state network $= (i, f)$, which is the combination of time point i and the SoC level of the EV fleet $f \in [1, L]$. We further define the state transition action as $a = (s, s') = (i, f, i', f')$. An example of state transition from time i to i' is shown in Fig. 2. The corresponding action reward for action $a \in A(s)$ is denoted as $r(a)$. Therefore, for charging operation the transition action is $a = a^c = (i, f, i+1, f+d^+)$ and the corresponding reward is $r(a^c) = c_i$. Similarly, the discharging action is $a = a^d = (i, f, i+1, f-d^-)$ and the reward is $r(a^d) = s_i$. The action of serving travel demand for time length $j \in \mathscr{J}$ is $a = a^t = (i, f, i+j, f-d_{ij})$ and the reward is $r(a^t) = b_{ij}$. Moreover, the action of staying idle is $a = a^0 = (i, f, i+1, f)$ and the reward is $r(a^0) = 0$.

With a given state distribution $\theta_s, s \in S$, a parameterized stochastic policy $\pi_\theta(a|s, \theta_s)$ is defined as the probability that action a is chosen. An exponential softmax distribution is applied to calculate the policy,

Table 1
Notation for key variables and parameters.

Parameters	Definition
$\mathscr{I}$	Set of time points, $I = \{1, ..., i, ..., I\}$
$\mathscr{J}_i$	Set of transportation service durations, $\mathscr{J}_i = \{1, 2, ..., j, ..., min\{J, I-i\}\}$
d_{ij}	Energy consumption for the fleet to serve demand during the time interval $[i, i+j], \forall i+j \in \mathscr{I}, \forall i \in \mathscr{I}, \forall j \in \mathscr{J}$
$\mathscr{K}_i$	Set of time point and transportation service duration pairs $(i' \in \mathscr{I}, j' \in \mathscr{J})$ such that the fleet will serve the transportation system at time point i; i.e., $\mathscr{K}_i := (i', j' \mid i' \in \mathscr{I}, j' \in \mathscr{J}, i' \le i \le i' + j' - 1), \forall i \in \mathscr{I}$
b_{ij}	Revenue of serving the transportation system during the time interval $[i, i+j], \forall i+j \in \mathscr{I}, \forall i \in \mathscr{I}, \forall j \in \mathscr{J}$
c_i	Charging cost during the time interval $[i, i+1], \forall i \in \mathscr{I}$
s_i	Revenue of discharging during the time interval $[i, i+1], \forall i \in \mathscr{I}$
d^+	Increase of state of charge (SoC) when charging in every time interval $[i, i+1], \forall i \in \mathscr{I}$
d^-	Decrease of SoC when discharging in every time interval $[i, i+1], \forall i \in \mathscr{I}$
L	Initial SoC of the EV fleet
Variables	
x_{ij}	Whether choose to serve the transportation system during the time interval $[i, i+j], \forall i+j \in \mathscr{I}, \forall i \in \mathscr{I}, \forall j \in \mathscr{J}$
y_i	Whether to charge the fleet at time point i, $\forall i \in \mathscr{I}$
z_i	Whether to discharge the fleet at time point i, $\forall i \in \mathscr{I}$
f_i	SoC at time point i, $\forall i \in \mathscr{I}$

$$\pi_\theta(a|s,\theta_s) = \frac{\exp(\theta_s \times \rho_a)}{\sum_{a' \in A(s)} \exp(\theta_s \rho_{a'})}, \tag{1}$$

where ρ_a is the rate of the current action a and $\rho_{a'}$ is the rate of the previous action a'. For the action of rebalancing distribution or serving travel demand, the rate is $\rho_{a^r} = \lambda_{i,j,t}$. For the action of charging, the rate is calculated as $\rho_{a^c} = C_i/\Delta - \lambda^c_{i,t}$. Similarly, the rate for discharging action is calculated as $\rho_{a^d} = D_i/\Delta - \lambda^d_{i,t}$.

The proportion of time that vehicles spend in the state s' with policy π_θ is formulated as $\eta_s = \sum_{s' \in S} \eta_{s'} \sum_a \pi_\theta(a|s',\theta_s) p(s,r|s',a)$ where $p(s,r|s',a)$ is the probability of transition from state s' to state s with action a and reward r. By parameterizing the time distribution, the on-policy distribution should be the fraction of time spent in each state to the sum of time spent in all states: $\mu_s = \frac{\eta_s}{\sum_{\bar{s} \in S} \eta_{\bar{s}}}$. The average reward thus can be calculated as follows (Sutton and Barto, 2017).

$$r(\pi_\theta) = \sum_{s' \in S} \mu_{s'} \sum_{a \in A(s)} \pi_\theta(a|s,\theta_s) \sum_{s' \in S, r} p(s,r|s',a) r(a). \tag{2}$$

To maximize the average reward, the differential action-value function is needed to calculate the gradient of Equation (7). It can be calculated by solving the following Bellman's equation (Sutton and Barto, 2018).

$$q_{\pi_\theta}(s,a) = \sum_{r,s'} p(s,r|s',a) \{ r(a) - r(\pi_\theta) + \sum_{a'} \pi_\theta(a'|s',\theta_{s'}) q_{\pi_\theta}(s',a') \} \tag{3}$$

where $q_{\pi_\theta}(s,a)$ and $q_{\pi_\theta}(s',a')$ are the expected differential returns of policy π for state-action pair (s,a) and (s',a') , respectively.

The gradient is calculated as follows.

$$\nabla J(\theta_s) = \sum_s \mu(s) \sum_a q_{\pi_\theta}(s,a) \nabla \pi(a|s,\theta_s) \tag{4}$$

The gradient is updated iteratively at each iteration ,

$$\theta_s^{k+1} = \theta_s^k + \alpha^k \nabla J(\theta_S^k) \tag{5}$$

To compute $\nabla J(\theta)$, we need the gradient of the softmax function $\pi(a|s,\theta_s)$, which is the partial derivative of the policy probability corresponding to the input s, which can be updated with the algorithm proposed in the next section.

3. Algorithm

We propose a customized dynamic programming (DP) method that is shown to be able to obtain the optimal state value and the optimal solution efficiently, even for large-scale instances. To apply DP to the proposed MDP model, we set each time point $i \in \mathscr{I}$ as a decision stage. At each stage i, with the state $s = f_i$ and the active space $a \in A(s)$, the state transition from stage i with state $s = f_i$ with action $a \in A(s)$ to $s' = f_{i+j}$ at stage $i+j$ is essentially determined by the change of SoC as written in the following state transfer function:

$$s' = f_{i+j} | s = f_i, a \in A(s) = \begin{cases} \min\{f_i + d^+, L\}, & \text{if } a = a^c; \\ f_i - d^-, & \text{if } a = a^d; \\ f_i, & \text{if } a = a^0; \\ f_i - d_{ij}, & \text{if } a = a^t, \end{cases} \forall a \in A(s) \tag{6}$$

Without the loss of generality, we set the final state $s = f_I$ is L in stage I, we may need to further reduce the action space as follows:

$$A(s = f_I) = \{ a = (i,f,i+j,f') \in A(s = f_i) | f' = L, \text{if } i+j = I \} \tag{7}$$

Besides, without the loss of generality, we set the state at time point $i = 0$ as $s = f_0 = L$. The state spaces in the remaining stages can be obtained with the following iterative state search (SC) algorithm:

SC-0: Set $s = f_0 = \{L\}, s = f_i = \varnothing, \forall i \in \mathscr{I}$ and $= 0$.

SC-1: For each $s = f_i \in S, a = (i,f_i,i+j,f_{i+j}) \in A(s)$, add $s = f_{i+j}$ into .

SC-2: If $i < I$, update $i = i+1$ and repeat SC-1; otherwise, return with $\theta_s, s = f_I = L$.

Note that due to the definition of $A(a)$ and Equation (7), the SC algorithm always yields $f_I = L$. With this, the associated benefit for each action in stage i is formulated as

$$r(a) = \begin{cases} -c_i, & \text{if } a = a^c; \\ s_i, & \text{if } a = a^d; \\ 0, & \text{if } a = a^0; \\ b_{ij}, & \text{if } a = a^t, \end{cases} \forall (action, j) \in A_i, i \in \mathscr{I} \{ \mathrm{I} \tag{8}$$

Let $B_i(s)$ be the optimal cumulative benefit from stage i through stage I conditioning on the stage at stage i is $s = f_i$, then with the corresponding Bellman equation, this problem can be solved with the following backward iteration (BI) algorithm:

BI-0: Set $B_I(L) = 0$ *and* $= I - 1$.

BI-1: Solve the following Bellman equation,

$$B_i(s = f_i) = \max_{a \in A(s)} \left\{ r(a) + B_{i+j}\left(f_{i+j}\right) | a = \left(i, f_i, i+j, f_{i+j}\right) \right\}, \forall s = f_i \in S$$

Let $a_i^*(B_i, B_{i+j})$ denote the optimal solution to the above equation.

BI-2: If $i > 0$, update $i = i+1$ and repeat BI-1; otherwise, initialize optimal decision set A^* and go to the next step to use a backward search to pinpoint the series of the optimal states and actions.

BI-3: Initialize the last state, optimal objective, and stage $i' = I,\ s = f_I = L,\ B_I(L),\ i' = I$.

BI-4: Get the last decision in $a_i^*(B_i, B_{i'})$, and append it into a set A^*.

BI-5: If $i > 0$, repeat BI-4; otherwise, return $B_i(L)$ as the optimal objective and A^* as the optimal decision, where each element $a \in A$ denotes that at stage i, the optimal SoC is $s = f$ and the optimal action is a^*.

4. Case studies

This section applies the proposed model to case studies with real-world shared mobility data. Section 4.1 describes the method on how to extract the parameters by processing real-world disaggregated taxi and power data. Section 4.2 compares the DP algorithm's performance with a commercial solver. Section 4.3 shows the detailed time allocation solutions for two benchmark instances. Section 4.4 conducts sensitivity analysis to draw insights into how parameter values affect the optimal operational policy. It is noted that the proposed approach does not limit to a specific EV sharing system, the presented procedure can be applied to any real-world instance as long as the required data is available.

4.1. Data-driven based simulation and computational environment

This section describes the procedure to obtain the parameters. Instead of making simple assumptions on the values of parameters, we set the values by processing massive real-world data. As we obtain demand revenue in the time dimension, we need to ensure that the spatial distribution of real-world travel demands is consistent with the values of transportation revenue parameters. To this end, we propose a data-driven-based EV sharing simulation method to prove the external validity of the revenue estimation.

The first data set is a set of trip records collected in the Taxicab & Livery Passenger Enhancement Programs for New York City (NYC) in January 2016. The investigated time horizon $\mathscr{I}$ is set to be a period within this month. This dataset is used to extract transportation revenue matrix $[b_{ij}]$ and electricity consumption matrix $[d_{ij}], \forall i \in I, \forall j \in J$. Since we intend to investigate an EV sharing system, we treat each taxi as an EV. The data set contains a total of 10,906,858 trips, denoted as $\mathscr{P}$, from a group of 13,587 yellow cab taxis. For each trip $p \in \mathscr{P}$, it records the pickup time, pickup location, drop-off time, drop-off location, and the corresponding taxi fare. Let t_p^0, t_p^1 denote pickup time and drop-off time. For a trip p associated with time window $[i, i+j]$ (or window ij for short), there are three possible cases: (i) admissible to window ij if this trip is completely enclosed within this window, *i.e.*, $i \le t_p^0, t_p^1 \le i+j$; (ii) intersecting with window ij if it crosses one window border, i.e., $t_p^0 < i < t_p^1 \le i + j or i \le t_p^0 < i+j < t_p^1$; or (iii) passing window ij if $t_p^0 < i and i + j < t_p^1$. Note that if we decide to dispatch the EV fleet to server travel demand in window ij in the proposed model, they can only serve trips admissible to window ij, and thus the relevant cost and revenue shall be referred only from these admissible trips. Let $\mathscr{P}_{ij}$ denote the set of all admissible trips to window ij. We assume that if the EV fleet is dispatched in window ij, they can only serve trips in $\mathscr{P}_{ij}$ but not other trips, even those intersecting with window ij. For each trip $p \in \mathscr{P}_{ij}$, we have the corresponding taxi fare in the data set, denoted by v_p, and the corresponding driving cost, denoted as v_p^0. This information is extracted from (NEWSROOM, 2016). With this, revenue b_{ij} can be estimated as the average revenue of admissible trip set $\mathscr{P}_{ij}$ during window ij, i.e., $\sum_{p \in \mathscr{P}_{ij}} \left(v_p - v_p^0 \right) / |\mathscr{P}_{ij}|$. Based on the trip distance hp for each trip p ∈ P in the data set, we can easily calculate the average trip distance within time window ij, i.e., $\bar{h}_{ij} = \sum_{p \in \mathscr{P}_{ij}} h_p / \mathscr{P}_{ij}$. For illustration purposes, we assume the configurations of an EV are the same as the Tesla Model S. Then with Tesla Model S's energy consumption rate per mile provided by the Environmental Protection Agency (Wikipedia, 2021), we can obtain d_{ij} as a product of this rate and the $\bar{h}_{ij}$ length.

To prove the external validity of demands revenue, we reproduce travel demands in NYC and simulate EV operations to serve the demands and calculate the average demand serving revenue. In the simulation system, we deploy a fleet of 3000 EVs in New York City to serve travel demands. The demand data are collected in the Taxicab & Livery Passenger Enhancement Programs for New York City (NYC) (NYC, 2016) on January 01, 2016. The time interval is 10 mins between each two consecutive time points $[i, i+1], \forall i \in \mathscr{I}$. The location data of charging stations in NYC are extracted from OpenData (NYC Open data, 2016). We consider the set of transportation service duration $\mathscr{J}_i$ at each time point i as $\mathscr{J}_i = \{1,2,3,4,5,6\}, \forall i \in \mathscr{I}$. In the beginning, the fleet of EVs is randomly distributed in charging stations. To estimate the average revenue of serving travel demands for a transportation service duration $j \in \mathscr{J}_i$, the fleet will serve travel demands in $\mathscr{P}_{ij}$, the set of all admissible trips in window ij. For each demand, it will be served by the nearest EV. If there are idle EVs at a certain time window ij, they will rebalance to the nearest charging stations and charge until the SoC of the EV reaches its capacity L or until time point $i+j$. In case that the SoC of an EV is less than 20 kWh, it will rebalance to charge for a time duration j in the nearest charging station. To estimate the average revenue to serve travel demands d_{ij} in time window ij, we calculate the sum of the revenue of the fleet in time window ij and divide it by the fleet size 3000. We operate the system 20 times and take the average value of d_{ij}. The resulting d_{ij} is \$14.332 while the average revenue calculated from the original dataset is \$14.858. The small difference verifies the effectiveness of the above configuration.

The second data set is the electricity rates in New York City, January 2016 (Pjm, 2016). This dataset together with the charging and discharging rates of Tesla Model S yields charging cost c_i and discharging price s_i for each interval $[i, i+1], i \in \mathscr{I}$. We can also obtain the increase of SoC for charging in one time interval, d^+, and the decrease of SoC for discharging at one time interval, d^-, and the initial battery level L .

Note that with different time discretization intervals and time horizon durations, we can populate data sets of different sizes. In the following experiments, we vary the discretization interval from 5 to 30 min and the time horizon from one day to the full month to generate a series of instances.

4.2. Model performance

In this section, we analyze the performance of the DP method proposed in Section 3. The algorithm is implemented with the Python language on a computer with a 3.60 GHz CPU, 16.0 GB RAM, and the Windows 7-x64 OS. We build the model with the data sets populated in Section 4.1. The results are summarized in Table 2. The considered time interval, denoted by t0 is 5 min, 10 min, 15 min, 20 min, and 30 min in time horizon T for 1, 2, 7, 15, 30 days. Therefore, the number of time intervals I is equal to $T \times 24 \times 60 / t_0$. As more than 95% of travel demands are completed in 60 mins, we set the maximum travel demand serving time as 60 min. In the table, we see that when the instance size increases, the DP solution time increases linearly and yields the optimal solution below one second for most cases and always no greater than 7 s. Overall, the proposed DP method can efficiently solve the problem and correspond to a more detailed representation of system dynamics and more flexible service options for the EV sharing system.

4.3. Comparison with benchmark

4.3.1. Comparison of time allocation solutions

In this section, we test the time allocation solutions to two benchmark instances by varying the revenue of serving the transportation system and the price of electricity in the power system. We set the default value of the time interval as 10 min and the time horizon as 30 days. In Fig. 3, we show the optimal time allocations at the first 24 time points in different scenarios. The choices of charging, discharging, serving the transportation system, and staying idle are labeled as S^c, S^d, S^t and S^i respectively.

In Fig. 3(a), we test the time allocation solution to instances with different revenue profiles of serving the transportation system. In the figure, the scenarios are populated by artificially varying the revenue profiles in the following way. We define the mean and variance coefficients of the revenue profile as r^b with a default value of 1 and v^b with a default value of 250, respectively, and then populate these scenarios with the following formula with various r^b and v^b:

$$b_{ij}^{'} = max\{0, r^b \times m^b + \varepsilon ij(v^b) - v^b\}, \forall i \in \mathscr{I}, j \in \mathscr{J}_i,$$

where m^b is the mean of the original transportation revenues, $m^b = \frac{\sum_{i \in \mathscr{I}, j \in \mathscr{J}_i} b_{ij}}{I \times J}$, $\varepsilon ij(v^b)$ is a number randomly populated following the Poisson distribution with variance v^b (and thus $\{\varepsilon ij(v^b)\}$ values across different indexes are populated independently), and we use the function max {} to ensure populated revenue $\left\{b_{ij}^{'}\right\}$ values being positive. In these instances, we choose r^b among {0.1, 1, 2.5} and v^b among {0, 250, 500} (2) to explore the impacts of different magnitudes and variances of transportation revenues (here, the mean transportation revenue m^b is 13.57 (\$) and variance values are set compatible to the default variance of revenue series $\{b_{ij}\}, i \in \mathscr{I}, j \in \mathscr{J}_i$, 247.32 (\$)). With this, in instances 'RS', 'LT', 'HT', 'LTV', 'HTV', the values for (r^b, v^b) are set to (1, 250), (0.1, 250), (2.5, 250), (1, 0) and (1, 500), respectively, and the default $\{b_{ij}\}$ values are replaced with the corresponding $\left\{b_{ij}^{'}\right\}$ values in each instance. This way, instance 'RS' captures the default transportation revenue scenario; instances 'LT' and 'HT' capture low and high transportation revenue scenarios, respectively; and instances 'LTV' and 'HTV' capture low and high transportation revenue variance scenarios, respectively.

Compared with benchmark instance 'RS', instances 'LT' and 'LTV' have shorter times allocated to the transportation system while instances 'HT' and 'HTV' have longer transportation service times, which indicates that the transpiration service time allocation increases with the transportation revenue magnitude and the variance of transportation revenues. A higher mean indicates a higher revenue per unit

Table 2
Comparison between dynamic programming and Gurobi.

Time horizon T (day)	Time interval t_0 (min)	Solution time (sec)	C^c (\$)	B^d(\$)	B^t(\$)	B(\$)
1	30	0.01	11.98	26.23	114.82	129.07
1	20	0.02	13.30	29.98	142.83	159.51
1	15	0.03	11.85	11.88	184.12	184.14
1	10	0.07	13.56	0.00	240.13	226.57
1	5	0.22	21.57	0.00	383.19	361.61
2	30	0.02	21.05	39.47	244.99	263.41
2	20	0.06	26.79	61.21	294.38	328.81
2	15	0.05	22.65	11.88	387.98	377.20
2	10	0.11	26.92	0.00	489.81	462.88
2	5	0.40	43.29	0.00	767.01	723.72
7	30	0.06	130.45	418.34	673.44	961.33
7	20	0.17	167.81	660.25	730.61	1223.05
7	15	0.21	157.02	555.87	950.42	1349.27
7	10	0.45	144.16	308.96	1431.97	1596.77
7	5	1.50	185.47	0.00	2712.56	2527.09
15	30	0.15	283.26	913.84	1443.64	2074.22
15	20	0.28	374.57	1494.52	1522.58	2642.54
15	15	0.49	335.76	1154.31	2089.75	2908.29
15	10	1.00	310.06	662.33	3127.68	3479.95
15	5	3.05	408.42	116.39	5708.48	5416.44
30	30	0.27	483.78	1489.69	2960.81	3966.72
30	20	0.54	620.13	2270.32	3412.32	5062.51
30	15	0.87	532.70	1469.46	4712.39	5649.15
30	10	1.83	510.45	680.25	6722.55	6892.35
30	5	6.30	768.48	123.32	11795.20	11150.03

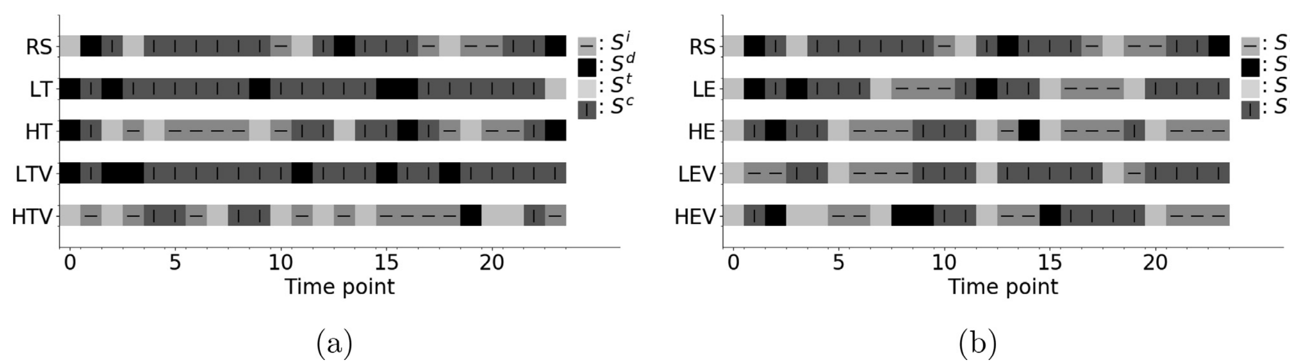

Fig. 3. Comparison of time allocation solutions: (a) varying transportation revenues; and (b) varying electric prices.

time, which intuitively draws longer transportation service times. When the variance is higher, the fleet may find more time intervals where the transportation revenues are higher than the power market returns and thus are more prone to the transportation market.

Fig. 3(b) shows the time allocation solutions to instances with different mean and variance values of electricity rates. We denote the mean and variance of the electricity rates as me with a default value of 30 (\$/KWh) and v^e with a default value of 200 (\$^{2}/KWh^2), respectively. Then these scenarios are populated with the following formula with various m^e and v^e values:

$$p_i^e = max\{0, m^e + \varepsilon_i(v^e) - v^e\}, \forall i \in \mathscr{I},$$

where p_i^e is the electricity rate at time point $\forall i \in \mathscr{I}, \varepsilon_i(v^e)$ is a number randomly populated following the Poisson distribution with variance v^e and function max{} is used to ensure p_i^e is positive. In these instances, we choose me among {20, 30, 40} and vb among {0, 200, 400}(\$^{2}) to explore the impacts of different magnitudes and variances of electricity rates. With this, in instances ‘RS’, ‘LE’, ‘HE’, ‘LEV’, ‘HEV’, the values for (m^e, v^e) are set to (30, 200), (20, 200), (40, 200), (30, 0) and (30, 400), respectively, and the default $\{s_i\}$ and $\{c_i\}$ values are replaced with the corresponding $\{p_i^e\}$ values in each scenario. This way, instance ‘RS’ captures the default electricity rate scenario; instances ‘LE’ and ‘HE’ capture low and high electricity rate scenarios, respectively; and instances ‘LEV’ and ‘HEV’ capture low and high electricity rate variance scenarios, respectively.

Comparing with benchmark instance ‘RS’, we see that the numbers of time intervals that the EV fleet is discharging in instances ‘LE’ and ‘HE’ are similar. However, instance ‘LEV’ has a shorter discharging time, and instance ‘HEV’ has a longer discharging time than instance ‘RS’. It is interesting to note that the mean of electricity rates does not likely influence the optimal time allocation. Actually, the increase in the mean electric price indicates that both charging cost and discharging income increase at the same magnitudes across all times, thus they offset each other during repeated discharging charging cycles – the fleet is not better off from a longer discharging, which has to be followed by a longer charging to maintain the power conservation in a long run. Whereas the variance of electricity rates obviously influences the optimal time allocation, as the fleet finds more opportunities for discharging at relatively high sale prices and charging at relatively low costs when the variance of electricity rates is higher.

4.3.2. Comparison of optimal total profits

In this section, we compared the optimal total profits of the EV sharing fleet providing discharging services with the optimal total profits of the EV fleet not providing discharging services to the power system. We set a time interval as 10 min and the time horizon as 30 days.

As shown in Fig. 4, we vary four crucial parameters in the system to compare the optimal total profit (denoted by B_{dis}) of the "energy sponge" service (i.e., with discharging services) and that (denoted by B_{nodis}) of the traditional shared EV service (i.e., without discharging services). These four figures obviously show that the "energy sponge" service can always yield much more profit at all parameter settings. For instance, as Fig. 4(c) shows, in nominal conditions, the "energy sponge" service improves the profit by over 40% on average. In Fig. 4(a), as transportation revenue mean coefficient r^b increases from 0.1 to 2.5, we see both services yield higher profits, yet their difference remains approximately the same. While increasing the transportation revenue obviously raises the total system profit, it is interesting to see that the profit difference is insensitive to the profitability of the transportation market alone. This indicates that even when the transportation market is quite profitable, introducing the "energy sponge" service remains beneficial. In Fig. 4(b), as the variance of the transportation revenue V^b increases from 0 to 500 ($\$^2$), both services have higher profits and their difference slightly increases as well. This indicates that it will be even more profitable to serve both transportation and power systems when the transportation market is more volatile. In Fig. 4(c), as the mean of electric rates m^e increases from 20 to 40 ($/KWh), the profits from both systems remain stable. This indicates that the profitability of both services is robust against systematic changes in the average electricity price. In Fig. 4(d), as the variance of electricity rate V^e increases from 0 to 400 ($\$^2/KWh^2$), we see that while the traditional shared EV service is not much impacted, the profit of the "energy sponge" service keeps increasing. This is because when the electricity rate varies more, there are more opportunities for the fleet to charge at lower costs and discharge at higher prices. It implies this new service will become more attractive as the power market gets more volatile.

4.4. Sensitivity analysis

In this section, we conduct the sensitivity analysis to test how the optimal time allocation and the optimal benefit change with different settings of transportation revenues and electricity rates. The default parameter values are consistent with Section 4.3. We set the time interval as 10 min and the time horizon as 30 days. The optimal time allocation solutions and revenue are shown in Fig. 5.

In Fig. 5(a and b), we test the influence of the magnitude of transportation revenues and set rb from 0.1 to 2.5. We see that the transportation service duration and the corresponding revenue both increase as rb grows. Again, this result verifies that a higher transportation revenue magnitude will make the transportation market preferable for longer times over the power market.

In Fig. 5(c and d), we vary the variance of transportation revenues vb from 0 to 500 ($2). We see that as the EV vb increases, the EV fleet serves the transportation system for a longer time while discharging for a shorter time, and the overall transportation revenue and the total benefit grow up. This again confirms that a higher transportation vari-

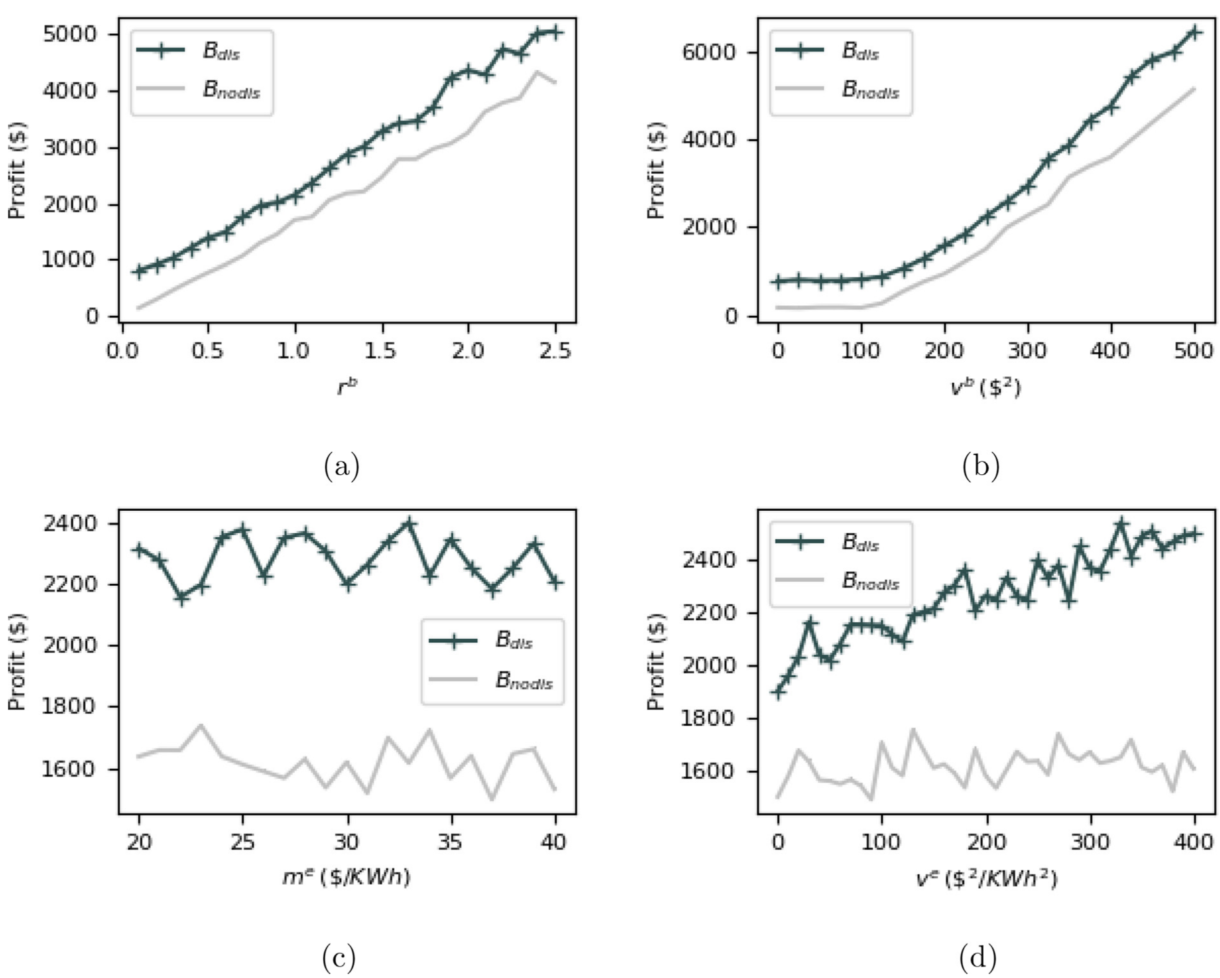

Fig. 4. Comparison of optimal total profits: (a) varying magnitude of transportation revenues; varying variance of transportation revenues; (c) varying mean of electric prices; and (d) varying variance of electric prices.

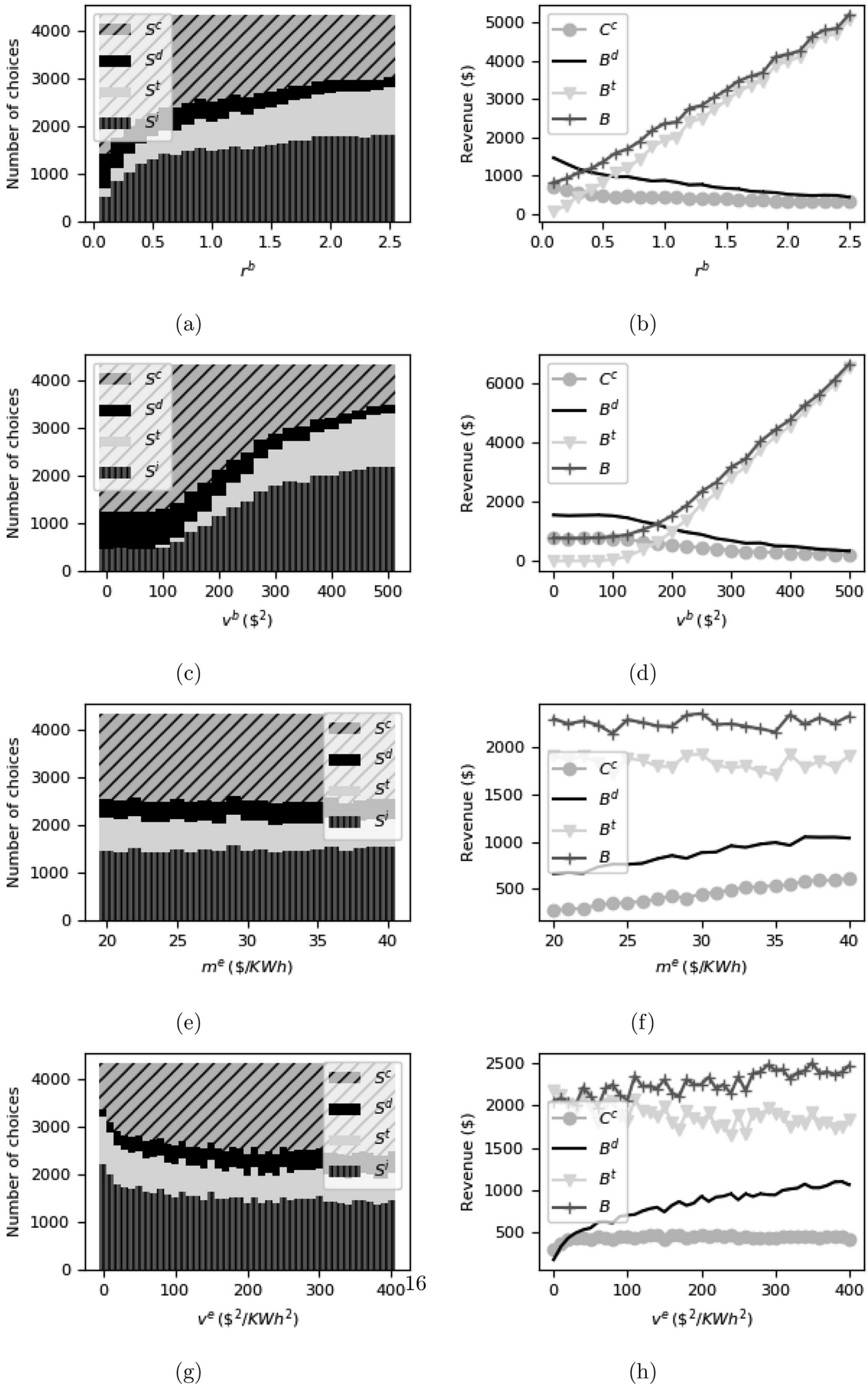

Fig. 5. Sensitivity analysis. (a), (b) varying magnitude of transportation revenues; (c), (d) varying variance of transportation revenues; (e), (f) varying mean of electric prices; (g), (h) varying variance of electric prices.

ance creates more opportunities to profit greater from the transportation market.

In Fig. 5(e and f), we change the mean of electricity rates me from 20 ($/KWh) to 40 ($/KWh). When me increases, the time allocations of different services do not change obviously and the total benefit neither varies much. The charging cost and the discharging revenue increase because of increased electricity rates. This shows that an overall shift of electricity rates does not much influence the optimal time allocation and the total benefit, again, due to the lack of creating electric price discrepancies across different times.

In Fig. 5(g and h), we change the variance of electricity rates ve from 0 to 400 ($2/KWh2). It is shown that the EV fleet discharges for a longer time and serves transportation for a shorter time when ve increases, and the overall discharging revenue and the total benefit increases with ve. This is consistent with the finding that a higher electric price variance creates more opportunities for higher electricity sale prices and cheaper charging costs across different times.

5. Conclusion and future research

This paper proposes the concept of an “energy sponge” for an EV sharing system that enables this system to serve both transportation and power markets. This concept can improve the carsharing system’s profitability by taking advantage of dynamics in both transportation and power markets. To realize this concept in time allocation decisions in an EV sharing system, we formulate an integer programming model and propose an efficient dynamic programming algorithm to solve it. We also propose a novel method to extract model input parameters from real-world data. The numerical example shows the high efficiency of the proposed DP algorithm regarding the solution time and the precision of optimal solutions and benefits. The sensitivity analysis reveals interesting insights into how the optimal time allocations and the benefit components change with the key parameter settings. We find that the system profit is improved by the proposed “energy sponge” service by over 40% on average in nominal conditions and is further amplified as the variances of the transportation revenue and the electricity price increase. Although this study focuses on optimizing the operation of shared EV fleets, the proposed methodology also has great potential in other logistics and supply chain systems where EVs are used to deliver goods or services.

The current model can be extended to several directions. First, it is interesting to consider spatial heterogeneity of the demand and EV distributions. Incorporating detailed routes of individual EVs (instead of a fleet as a whole) based on spatially distributed travel demands can further improve the system efficiency and reduce its costs. Second, the current model assumes future travel demand and the price of electricity are known in advance. While this assumption suffices for certain planning purposes, it may not satisfy real-time operation needs. This can be addressed by integrating travel demand and electricity rate prediction models into this study. Last, while the current model focuses on the profitability of the EV fleet alone, it is also important to investigate how to utilize the “energy sponge” service in dampening the oscillations in both transportation and power markets and enhancing the resilience of both systems.

Declaration of Competing Interest

The authors declare that they have no known competing financial interests or personal relationships that could have appeared to influence the work reported in this paper.

Acknowledgment

This research is supported by the US National Science Foundation through Grants CNS #1638355 and #1637772.

References

Alizadeh, M., Wai, H.T., Scaglione, A., Goldsmith, A., Fan, Y.Y., and Javidi, T., 2014. Optimized path planning for electric vehicle routing and charging, *in: Communication, Control, and Com- puting (Allerton), 2014 52nd Annual Allerton Conference on*, IEEE, 25–32.

Asamer, J., Reinthaler, M., Ruthmair, M., Straub, M., Puchinger, J., 2016. Optimizing charging station locations for urban taxi providers. Transportation Research Part A: Policy and Practice 85, 233–246.

Bai, J., SO, K.C., Tang, C., Chen, X., and Hai, W., 2017. Coordinating supply and demand on an on-demand platform: Price, wage, and payout ratio.

Bardaka, E., Hajibabai, L., Singh, M.P., P. Singh, M., K. Murukannaiah, P., 2020. Reimagining Ride Sharing: Efficient, Equitable, Sustainable Public Microtransit. IEEE Internet Computing 24 (5), 38–44.

Becker, T.A., Sidhu, I., Tenderich, B., 2009. In: Electric vehicles in the United States: a new model with forecasts to 2030. University of California, Berkeley, Center for Entrepreneurship and Technology, p. 24.

Bimpikis, K., Candogan, O., and Daniela, S., 2016. Spatial pricing in ride-sharing networks.

Britton, E., 2000. Carsharing 2000: Sustainable transport’s missing link. Eco-Logica.

Cachon, G.P., Daniels, K.M., Lobel, R., 2017. The role of surge pricing on a service platform with self-scheduling capacity. Manufacturing and Service Operations Management 19 (3), 368–384.

Caggiani, L., Prencipe, L.P., Ottomanelli, M., 2021. A static relocation strategy for electric car-sharing systems in a vehicle-to-grid framework. Transportation Letters 13 (3), 219–228.

Cao, Y., Tang, S., Li, C., Zhang, P., Tan, Y.i., Zhang, Z., Li, J., 2012. An optimized EV charging model considering TOU price and SOC curve. IEEE Transactions on Smart Grid 3 (1), 388–393.

Chen, T.D., Kockelman, K.M., Hanna, J.P., 2016a. Operations of a shared, autonomous, electric vehicle fleet: Implications of vehicle & charging infrastructure decisions. Transportation Research Part A: Policy and Practice 94, 243–254.

Chen, Z., He, F., Yin, Y., 2016b. Optimal deployment of charging lanes for electric vehicles in transportation networks. Transportation Research Part B: Methodological 91, 344–365.

Du, G., Cao, W., Yang, J., Zhou, B., 2016. An optimization model of EVs charging and discharg- ing for power system demand leveling. In: Power and Energy Engineering Conference (APPEEC), 2016 IEEE PES Asia-Pacific. IEEE, pp. 835–842.

Ford, A., 1995. The impacts of large scale use of electric vehicles in southern California. Energy and Buildings 22 (3), 207–218.

Gao, S., Chau, K.T., Liu, C., Wu, D., Chan, C.C., 2014. Integrated energy management of plug- in electric vehicles in power grid with renewables. IEEE Transactions on Vehicular Technology 63 (7), 3019–3027.

Gardner, L.M., Duell, M., Waller, S.T., 2013. A framework for evaluating the role of electric vehicles in transportation network infrastructure under travel demand variability. Transportation Research Part A: Policy and Practice 49, 76–90.

Gardner, L.M., Unnikrishnan, A., Waller, S.T., 2010. Solution methods for robust pricing of transportation networks under uncertain demand. Transportation Research Part C: Emerging Technologies 18 (5), 656–667.

Gminsights, 2020. Car Sharing Market.

Green, C., 2009. Car-Sharing – Good for the Environment and the Budget

Guda, H. and Subramanian, U., 2017. Strategic Pricing and Forecast Communication on On-Demand Service Platforms.

Guo, Z., Lei, S., Wang, Y., Zhou, Z., Zhou, Y., 2017. Dynamic distribution network reconfig- uration considering travel behaviors and battery degradation of electric vehicles. In: 2017 IEEE Power and Energy Society General Meeting. IEEE, pp. 1–5.

He, F., Wu, D.i., Yin, Y., Guan, Y., 2013. Optimal deployment of public charging stations for plug-in hybrid electric vehicles. Transportation Research Part B: Methodological 47, 87–101.

He, F., Yin, Y., Lawphongpanich, S., 2014. Network equilibrium models with battery electric vehicles. Transportation Research Part B: Methodological 67, 306–319.

He, Y., Venkatesh, B., Guan, L., 2012. Optimal scheduling for charging and discharging of electric vehicles. IEEE transactions on smart grid 3 (3), 1095–1105.

Huang, Y., Li, S., Qian, Z.S., 2015. Optimal deployment of alternative fueling stations on transportation networks considering deviation paths. Networks and Spatial Economics 15 (1), 183–204.

Jiao, Z., Ran, L., Zhang, Y., Ren, Y., 2021. Robust vehicle-to-grid power dispatching operations amid sociotechnical complexities. Applied Energy 281, 115912. https://doi.org/10.1016/j.apenergy.2020.115912.

Juul, N. and Meibom, P., 2011. Optimal configuration of an integrated power and transport system, *Energy*, 36 (5), 3523–3530.

Koyanagi, F., Uriu, Y., 1998. A strategy of load leveling by charging and discharging time control of electric vehicles. IEEE Transactions on Power Systems 13 (3), 1179–1184.

Li, S., Huang, Y., Mason, S.J., 2016a. A multi-period optimization model for the deployment of public electric vehicle charging stations on network. Transportation Research Part C: Emerging Technologies 65, 128–143.

Li, X., Ma, J., Cui, J., Ghiasi, A., Zhou, F., 2016b. Design framework of large-scale one-way electric vehicle sharing systems: A continuum approximation model. Transportation Research Part B: Methodological 88, 21–45.

Mahmoudi, M., Zhou, X., 2016. Finding optimal solutions for vehicle routing problem with pickup and delivery services with time windows: A dynamic programming approach based on state–space–time network representations. Transportation Research Part B: Methodological 89, 19–42.

Martin, E., Shaheen, S.A., Lidicker, J., 2010. Impact of carsharing on household vehicle holdings: Results from North American shared-use vehicle survey. Transportation Research Record: Journal of the Transportation Research Board 2143 (1), 150–158.

Martin, E.W., Shaheen, S.A., 2011. Greenhouse gas emission impacts of carsharing in North America. IEEE Transactions on intelligent transportation systems 12 (4), 1074–1086.

NEWSROOM, 2016. Driving Cost Per Mile.

Nie, Y.M., Liu, Y., 2010. Existence of self-financing and Pareto-improving congestion pricing: Impact of value of time distribution. Transportation Research Part A: Policy and Practice 44 (1), 39–51.

NYC, 2016. TLC Trip Record Data.

NYC Open data, 2016. NYC Street Centerline.

Ortega-Vazquez, M.A., Bouffard, F., Silva, V., 2013. Electric vehicle aggregator/system opera- tor coordination for charging scheduling and services procurement. IEEE Transactions on Power Systems 28 (2), 1806–1815.

Parsons, G.R., Hidrue, M.K., Kempton, W., Gardner, M.P., 2014. Willingness to pay for vehicle- to-grid (V2G) electric vehicles and their contract terms. Energy Economics 42, 313–324.

Pjm, 2016. Energy Market

Quddus, Md Abdul, Kabli, Mohannad, Marufuzzaman, Mohammad, 2019. Modeling electric vehicle charging station expansion with an integration of renewable energy and Vehicle-to-Grid sources. Transportation Research Part E: Logistics and Transportation Review 128, 251–279.

Ren, Shuyun, Luo, Fengji, Lin, Lei, Hsu, Shu-Chien, LI, Xuran Ivan, 2019. A novel dynamic pricing scheme for a large- scale electric vehicle sharing network considering vehicle relocation and vehicle-grid-integration. International Journal of Production Economics 218, 339–351.

Siddiqi, U.F., Shiraishi, Y., Sait, S.M., 2011. Multi constrained route optimization for electric vehicles using SimE. In: Soft Computing and Pattern Recognition (SoCPaR), 2011 International Conference of IEEE. IEEE, pp. 376–383.

Sovacool, Benjamin K., Axsen, Jonn, Kempton, Willett, 2017. The Future Promise of Vehicle-to-Grid (V2G) Integration: A Sociotechnical Review and Research Agenda. Annual Review of Environment and Resources 42 (1), 377–406.

Statista, 2020. Worldwide number of battery electric vehicles in use from 2016 to 2020.

Sundstrom, Olle, Binding, Carl, 2012. Flexible charging optimization for electric vehicles considering distribution grid constraints. IEEE Transactions on Smart Grid 3 (1), 26–37.

Taylor, T., 2017. On-demand service platforms.

Thiel, Christian, Perujo, Adolfo, Mercier, Arnaud, 2010. Cost and CO 2 aspects of future vehicle options in Europe under new energy policy scenarios. Energy policy 38 (11), 7142–7151.

Tu, Wei, Li, Qingquan, Fang, Zhixiang, Shaw, Shih-lung, Zhou, Baoding, Chang, Xiaomeng, 2016. Optimizing the locations of electric taxi charging stations: A spatial–temporal demand coverage approach. Transportation Research Part C: Emerging Technologies 65, 172–189.

Ukkusuri, Satish V., Mathew, Tom V., Waller, S. Travis, 2007. Robust transportation network design under demand uncertainty. Computer-Aided Civil and Infrastructure Engineering 22 (1), 6–18.

Wang, Yusheng, Huang, Yongxi, Xu, Jiuping, Barclay, Nicole, 2017. Optimal recharging scheduling for urban electric buses: A case study in Davis. Transportation Research Part E: Logistics and Transportation Review 100, 115–132.

Wikipedia, 2021. Tesla Model S.

Yi, Zonggen, Bauer, Peter H., 2016. Optimization models for placement of an energy-aware electric vehicle charging infrastructure. Transportation Research Part E: Logistics and Transportation Review 91, 227–244.

Yin, Yafeng, Madanat, Samer M., Lu, Xiao-Yun, 2009. Robust improvement schemes for road networks under demand uncertainty. European Journal of Operational Research 198 (2), 470–479.

Zhang, Y., Lu, M., Shen, S., 2021. On the values of vehicle-to-grid electricity selling in electric vehicle sharing. Manufacturing and Service Operations Management 23 (2), 488–507.